

Integrated View of Disruption Dynamics on Internal Electromagnetic and Plasma Structures in the Small Tokamak HYBTOK-II

M. Okamoto 1), S. Takamura 1), N. Ohno 2), S. Kajita 1), Y. Kikuchi 3), Y. Uesugi 4), T. Ozeki 5), Y. Kawano 5), M.Sugihara 6)

1) Graduate School of Engineering, Nagoya University, Nagoya 464-8603, Japan

2) EcoTopia Science Institute, Nagoya University, Nagoya 464-8603, Japan

3) Graduate School of Engineering, University of Hyogo, Hyogo 671-2280, Japan

4) Faculty of Engineering, Kanazawa University, Kanazawa 920-8667, Japan

5) Japan Atomic Energy Agency, Ibaraki 311-0193, Japan

6) ITER International Team, Naka Joint Work Site, Ibaraki 311-0193, Japan

e-mail: m-okamoto@ees.nagoya-u.ac.jp

Abstract. Integrated view of disruption dynamics on internal electromagnetic and plasma structures with a high time resolution is presented systematically. Main results are as follows: (i) Observation of electron temperature oscillation due to rotation of the magnetic island of $m/n = 3/2$ mode before the current quench and (ii) finding of rapid pump-out ($\sim 10 \mu\text{s}$) of plasma current and particles from the central core region just at current quench start time and then returning to a peaked profile during slow decay phase, and (iii) new proposal for the evaluation of current quench time and electron temperature dependence in the current quench time, so called τ/S scaling.

1. Introduction

The tokamak disruption, which is accompanied by an intense heat load on the divertor during thermal quench and a large electromagnetic force on in-vessel components during current quench, is one of the most crucial issues for the next generation tokamak, like ITER [1]. The internal measurement of disruptive plasma is very important to understand the physical processes involved in the disruption. In the experiment of medium and large size tokamaks, the inside of plasma is diagnosed with some contact-free methods like spectroscopic measurement because of a high plasma temperature. However, the electron temperature is too low to be measured after the current quench with conventional ECE technique. The electron temperature after thermal quench is so important parameter to evaluate plasma current decay time during current quench. On the other hand, these difficulties can be solved in small tokamaks with an advantage of inserting probes inside the plasma. The fast phenomenon during disruption and the electron temperature after thermal quench are fully accessible. In the old small tokamaks as TOSCA and LT-3, the internal magnetic field during disruption has been measured with magnetic probe without any sufficient recognition of thermal quench, current quench and current decay phase [2].

In this paper, the dynamical evolution of internal plasma structure is measured by the triple probe inserted into the small tokamak HYBTOK-II in addition to the magnetic probe array with a sufficient physical understanding of integrated physical image of disruption and an application to ITER including the establishment of scaling of current decay time. The feature

of this paper is comprehensive and integrative study of dynamic behaviour of disruptive plasma.

2. Waveform of disruption in HYBTOK-II

2.1 Experimental setup

HYBTOK-II is a small tokamak with a circular cross-section of limiter configuration. The major radius R and minor one a are 40 cm and 11 cm, respectively[3]. The device is equipped with an insulated gate bipolar transistor (IGBT) inverter power supplies for Joule as well as vertical field coils so that plasma current and the horizontal position of plasma column may be well controlled by a priori specified waveform. In order to demonstrate disruption, the IGBT inverter power supply for Joule circuit is switched to a condenser bank during a discharge in order to avoid an unnecessary power input from the IGBT power supply during disruption. Real-time feedback control of the plasma horizontal position makes it possible to enhance the reliability of the observations.

The triple probe and the magnetic probe were inserted vertically along the minor radius up to $r = 5$ cm from the bottom. Two kinds of magnetic probes were employed to measure internal magnetic field. One has two pick-up coils to measure radial and poloidal magnetic field. The other one is multi-channel probe to measure the profile of poloidal magnetic field at the same time. This probe has 10 pick-up coils with a spatial resolution of 7 mm.

2.2 New evaluation method of current quench time

The typical example of a discharge waveform with disruption is shown in Fig. 1. Disruption was driven by ramping up the plasma current I_p to reduce the plasma surface safety factor $q_a (= aB_t/RB_\theta)$ where B_t and B_θ are toroidal and poloidal magnetic field strength. In the experiment, the current quench occurred at $q_a < 3$ and, a negative spike of the plasma loop voltage V_{loop} was observed. The waveform of plasma current quench was found to have two phases of slow and fast decays.

In the database of current quench time in several tokamaks, the current quench time τ normalized to the plasma cross-section area S is plotted as a function of the average current density before a plasma current quench. From the database, the minimum value of τ/S has been evaluated. In the ITER design, the τ/S of $1.8 \sim 2$ ms/m² was

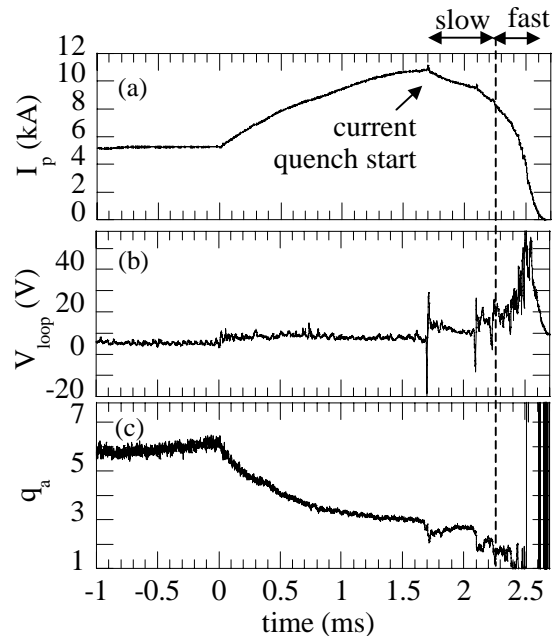


FIG. 1. Typical disruption waveform in HYBTOK-II ($B_t \sim 0.25$ T). Temporal evolutions of (a) plasma current I_p , (b) plasma loop voltage V_{loop} and (c) plasma surface safety factor q_a .

used. In classical consideration, τ could be determined by L_p/R_p where L_p is the plasma inductance and R_p is the plasma resistance, which leads to $\tau/S \propto T_e^{3/2}$ because R_p can be given by $R\eta/S$ and L_p is mainly determined by geometrical factor. Then, τ/S would have a weak dependence of device dimension, and the precise measurement of T_e is a key to understand the current quench time. On the other hand, the ambiguity of definition of τ from the plasma current waveforms gave a large scattering in the database. For instance, waveforms of current quench have a long tail due to runaway electrons caused by disruption. In order to reduce uncertainty and ambiguity for evaluation τ from a variety of plasma current waveforms, we have proposed a new definition of τ [4], in which both dI_p/dt corresponding to magnitude of electromagnetic force induced by current quench and the mechanical impulse on the vacuum vessel were taken into account. We defined current quench time τ_{proposed} as the time-width which gives 60 % of the whole plasma current around the time having maximum $|dI_p/dt|$ value, as shown in Fig. 2.

3. Experimental result

3.1 Growth of tearing mode

Figure 3(a), (b) and (c) show the temporal evolutions of the plasma current, the radial magnetic field B_r and the electron temperature T_e at $r = 5.5$ cm, respectively. As increasing the plasma current, the amplitude of B_r oscillation increases as shown in Fig. 3(b). We note that the oscillation of T_e is synchronized with that of B_r , especially during period of strong B_r oscillation.[5, 6] Figure 4(a) shows the amplitude profile of the radial magnetic field fluctuation and q profile. The B_r fluctuation would appear as $m/n = 3/2$ tearing mode because the amplitude of B_r fluctuation has a peak around $q = 1.5$ surface and $m = 3$ is confirmed from the poloidal mode analysis by the poloidally located external magnetic probe array. In Fig. 4, the magnetic island width can be evaluated by using the follow equation[7]:

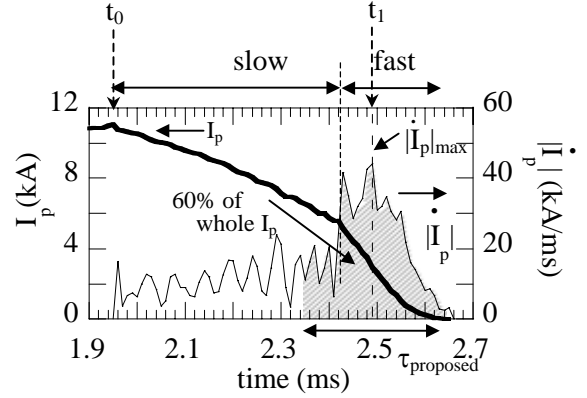


FIG. 2. Temporal evolutions of plasma current and its derivative during current quench in HYBTOK-II. Current quench starts at $t = t_0$. $|dI_p/dt|$ becomes maximum at $t = t_1$.

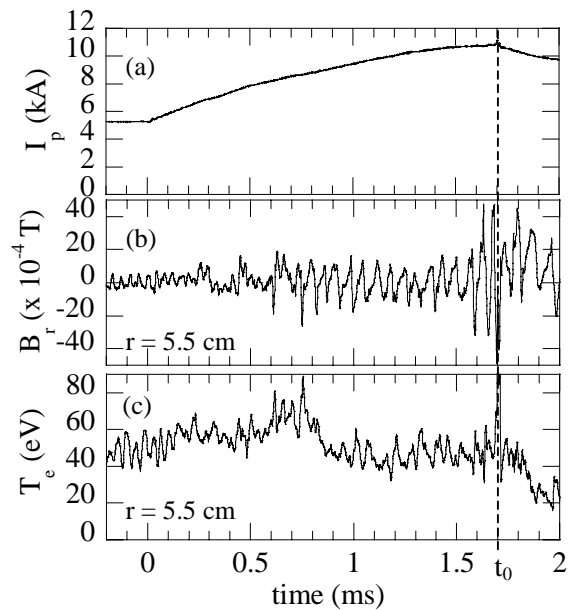


FIG. 3. Temporal evolutions of (a) plasma current, (b) radial magnetic field B_r at $r = 5.5$ cm., (c) electron temperature T_e at $r = 5.5$ cm. Current quench starts at $t = t_0$.

$$w = 4 \sqrt{\frac{rq\tilde{B}_r}{mq'B_\theta}},$$

where the minor radius $r \sim 6$ cm, the radial magnetic field amplitude $\tilde{B}_r \sim 15 \times 10^{-4}$ T, the poloidal magnetic field $B_\theta \sim 0.025$ T and the radial derivative of $q' \sim 28$ m⁻¹. The magnetic island width generated by $m/n = 3/2$ tearing mode is estimated about 3.2 cm. It is confirmed that the correlation between T_e and B_r fluctuations is large and the frequency of T_e fluctuation coincides with that of B_r fluctuation as shown in Fig. 4(b). The typical frequency of these fluctuations is about 16 kHz and the frequency was almost constant in all measured positions. Consequently, it is considered that T_e fluctuation could be induced by $m/n = 3/2$ magnetic island rotation. In Fig. 4(c), it is found that B_r and T_e fluctuations become antiphase around $r/a \sim 0.6$. By taking into account of the measurement positions of triple and magnetic probe separated by 45 degree in the toroidal direction, and assuming toroidal mode number is 2, the phase difference of T_e and B_r fluctuation corresponds to 90 degree at same poloidal cross-section. In Fig. 5, B_r fluctuation may be taken to have the form

$$B_r = \tilde{B}_r(r) \sin m\theta.$$

On the other hand, T_e becomes a maximum at O-point a minimum at X-point. The phase difference between T_e and B_r fluctuation induced by magnetic island rotation should be 90 degree, which is consistent with experimental observation.

3.2 Dynamics of disruptive plasma during current quench

Figure 6(a), (b) show the detailed time traces of the plasma current and the internal poloidal magnetic field B_θ at $r = 5.5$ cm around the moment of current quench starting time. Current profiles j_ϕ can be reconstructed by Ampere's law as shown in Fig. 6(c). It is found that the

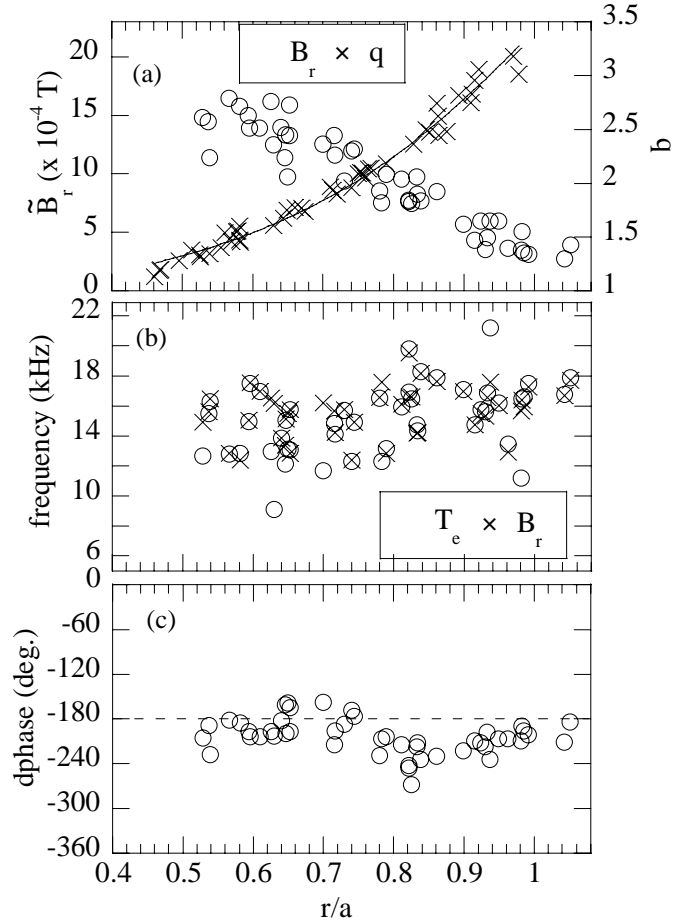


FIG. 4. (a) Amplitude profile of the radial magnetic field fluctuation and q profile. These profiles correspond to the time averaged profile over 0.4 ms between $t_0 - 0.4$ and t_0 ms. t_0 means current quench initiation time. (b) Frequency profiles, which are FFT analysis between $t_0 - 0.4$ and t_0 ms, of electron temperature and radial magnetic field fluctuation. (c) Phase difference between electron temperature and radial magnetic field oscillations.

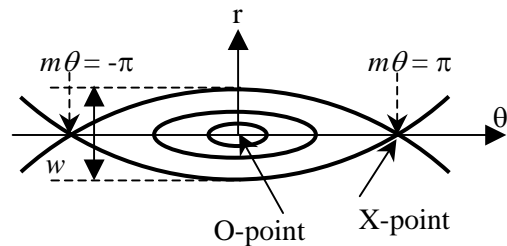


FIG. 5. Geometry of magnetic field lines of a magnetic island. w corresponds to the magnetic island width.

profile becomes suddenly flattened due to a rapid and strong pump-out ($\sim 10 \mu\text{s}$) of plasma current in the core region. Such a rapid pump-out could be caused by growth of $m/n = 3/2$ mode. In addition, the internal kink instability would appear because the q value near the center becomes less than unity just before current quench as shown in Fig. 4(a). After a pump-out of plasma current, a plasma confinement recovers later on and the profile gradually returns back to a peaked one during the slow decay phase.

Figure 7 shows the temporal evolutions of the plasma current and the electron density n_e at $r = 5.5 \text{ cm}$, and the electron density profiles around the current quench starting time ($t = t_0$). In the core region, n_e drops at $t = t_0$ and n_e increases at the edge, leading to a flattening of plasma density. The result suggests that a convective pump-out of plasma particles from core to edge regions occurs due to the magnetic connection between interior and edge through stochastic magnetic field[8]. Temporal evolution of the plasma current and the electron

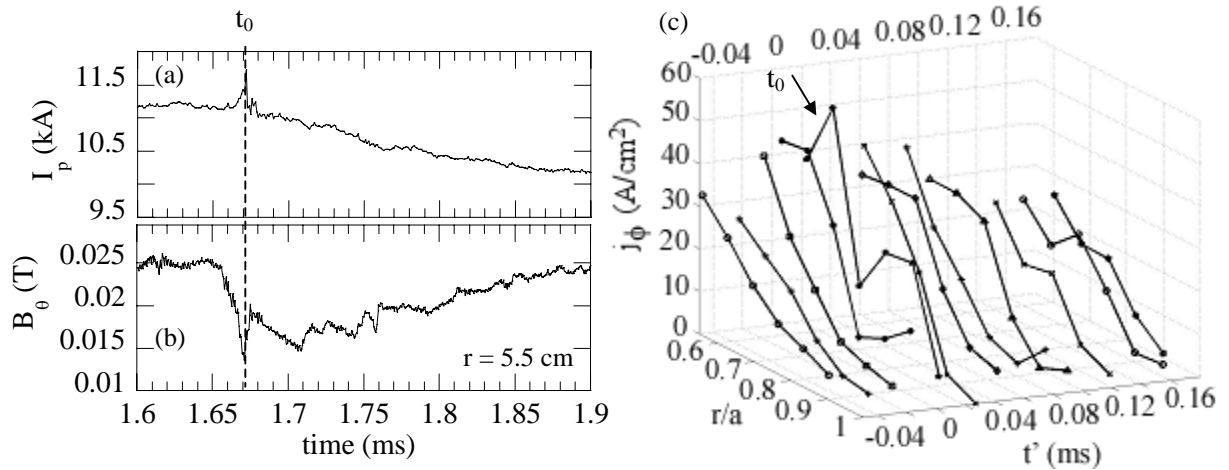


FIG. 6. Time traces of (a) plasma current, (b) poloidal magnetic field at $r = 5.5 \text{ cm}$ around current quench start time. (c) Temporal evolution of plasma current density profiles reconstructed from poloidal magnetic field measured by the multi-channel magnetic probe. $t' = 0 \text{ ms}$ corresponds to current quench start time ($t = t_0$).

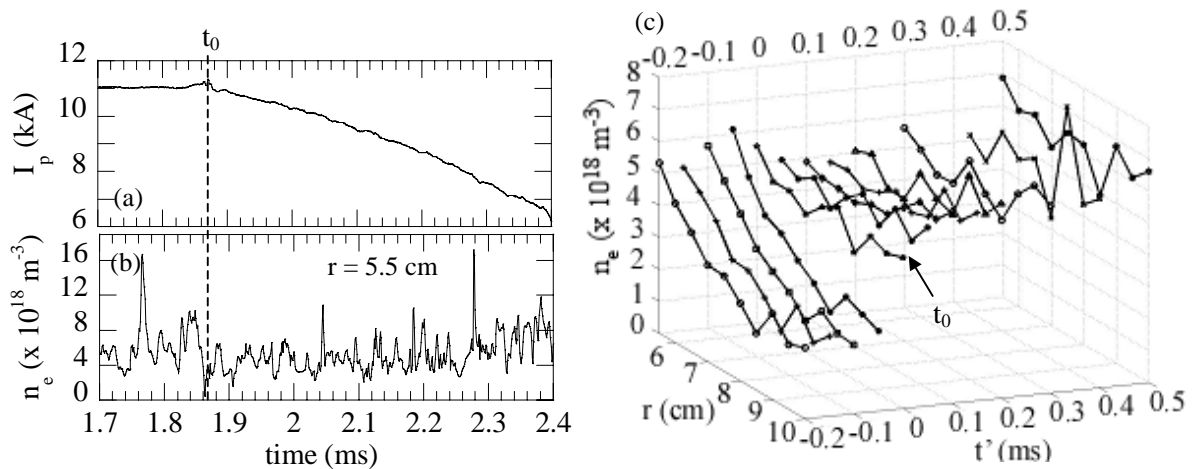


FIG. 7. Time traces of (a) plasma current, (b) electron density at $r = 5.5 \text{ cm}$ around current quench starting time. (c) Temporal evolution of the electron density profiles. The data points are obtained by averaging over the time window of $60 \mu\text{s}$. $t' = 0 \text{ ms}$ corresponds to current quench starting time.

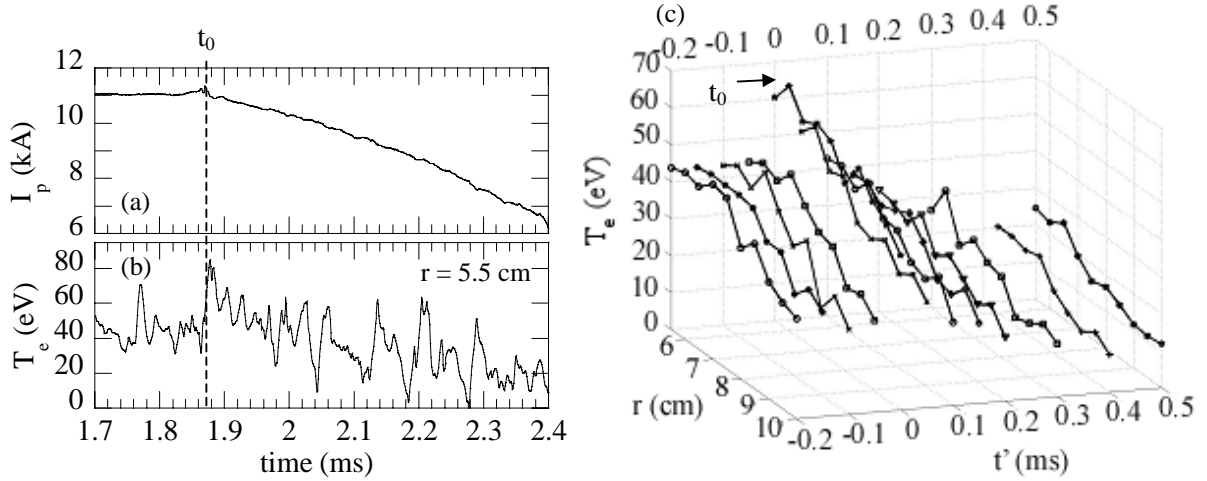


FIG. 8. Time traces of (a) plasma current, (b) electron temperature at $r = 5.5$ cm around current quench starting time. (c) Temporal evolution of the electron temperature profiles. The data points are obtained by averaging over the time window of $60 \mu\text{s}$. $t' = 0$ ms corresponds to current quench starting time.

temperature T_e at $r = 5.5$ cm, and electron temperature profiles around current quench starting time are also shown in Fig. 8. It is found that T_e increases at $t = t_0$, probably because hot core plasma in $r/a < 0.5$ was transported to the edge region although there is no T_e measurements at $r/a < 0.5$. Figure 9 shows temporal evolutions of line averaged T_e , n_e calculated from Fig.7(c) and Fig. 8(c) over the plasma edge, and the plasma resistivity η obtained by Spitzer formula[9]. After the start of slow decay phase, n_e increases until fast decay phase and start to decrease at the onset of fast decay phase. On the other hand, T_e is monotonically decreasing during both slow and fast decay phases although T_e increases rapidly at starting time of the slow decay phase. Finally T_e falls to be less than 10 eV in the fast decay phase. The strong T_e dependence is a reason why we have a steep increase of electrical resistivity of toroidal plasma.

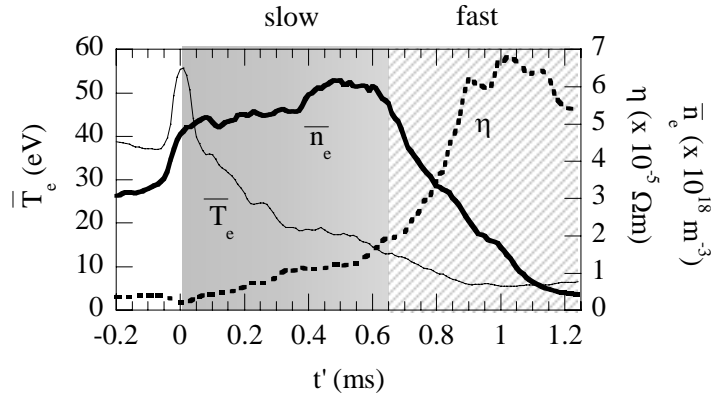


FIG. 9. Temporal evolution of line averaged electron temperature, density and plasma resistivity during current quench. $t' = 0$ ms corresponds to current quench starting time.

3.3 Evaluation of current quench time

We have applied new definition of current quench time proposed by us to disruption waveforms in HYBTOK-II. In Fig. 10, plots of averaged plasma current density $j_p = I_p/S$ against normalized decay time τ/S , are shown for comparing two different definition of decay time; time-width for plasma current decreasing from 80 % of whole current to 20 % (τ_{80-20}), which has been used in ASDEX-U and C-Mod tokamaks, and the proposed current

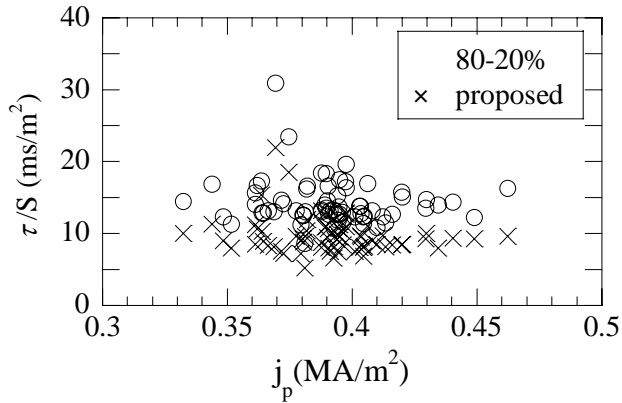


FIG. 10. Normalized current quench time compared between τ_{80-20} and $\tau_{proposed}$ as a function of plasma current density before current quench. S is the plasma cross-section area just before current quench.

quench time $\tau_{proposed}$. It is found in Fig. 8 that the data plots based on the conventional definition gives a rather larger scattering of τ/S to compare with new criterion because dispersions of τ_{80-20} and $\tau_{proposed}$ are 9.9 and 6.5, respectively.

Since waveforms of current quench in HYBTOK-II have two phases of slow and fast decays as shown before. The proposed current quench time has more strongly influenced by the waveform in the fast decay phase than that in the slow decay phase.

Figure 11 shows normalized decay time as a function of the electron temperature at $r = 5$ cm. It is found that the minimum value of τ/S is about 5 ms/m^2 around $T_e = 5 \sim 10 \text{ eV}$. The experimental observation is consistent with database of ITER. It seems that the decay times of slow and fast decay phase in HYBTOK-II depend on the average electron temperature.

4. Summary

The two important information on the dynamics of internal structure have been observed just before the current quench: the electron temperature oscillation due to magnetic island rotation of $m/n = 3/2$ mode and the q profile showing less than unity near the center. It is reasonability speculated that the sudden pump-out of the plasma current and particles at slow decay starting time is caused by the magnetic field line connection between the core and edge region though a stochastic magnetic layer due to a nonlinear interaction between $m/n = 1/1$ internal kink mode and $m/n = 3/2$ tearing modes. In a later phase of slow decay period, it is found that a plasma confinement is recovered and the electron density increases, but the electron temperature decreases in time.

We have proposed a new definition of current quench time and it is indicated that the

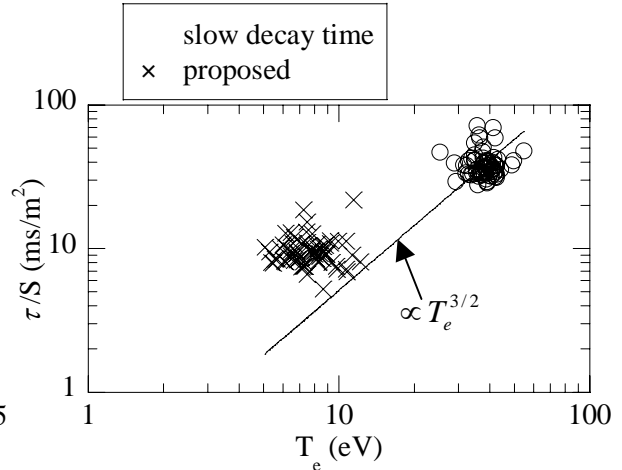


FIG. 11. Normalized current quench time as a function of electron temperature at $r = 5$ cm. Slow decay time corresponds to decay time calculated from the plasma current gradient between t_0 and $t_0 + 0.2$ and electron temperature corresponds to the time averaged over 0.2ms between t_0 and $t_0 + 0.2$ ms. t_0 means current quench starting time. The electron temperature of crosses corresponds to time averaged over 0.12 ms time period centered at t_1 which means the timing when $|dI_p/dt|$ reaches maximum as shown in Fig. 2.

proposed criterion have a smaller scatter of decay time than current criterion in HYBTOK-II. In addition, a scaling of current decay time as a function of electron temperature is experimentally shown.

Acknowledgements

The research was financially supported by the Sasakawa Scientific Research Grant from The Japan Science Society.

References

- [1] ITER Physics Basis, Nuclear Fusion, **39** (1999) 2251, chapter 3.
- [2] D.C. Robinson, K.M. McGuire, Nuclear Fusion, **19** (1979) 115.
- [3] S. Takamura *et al.*, Nuclear Fusion, **43** (2003) 393.
- [4] S. Kokubo *et al.*, Proceedings of 31st EPS Conference on Plasma Physics, London, 28 June - 2 July, 2004 ECA Vol. **28G**, P-2.137.
- [5] R. Fitzpatrick, Phys. Plasmas **2**, (1995) 825.
- [6] P. C. de Vries *et al.*, Plasma Phys. Controlled Fusion **39**, (1997) 439.
- [7] J.A. Wesson 1997 *Tokamaks* 3rd edition (New York: Oxford University Press) chapter 7, p 351,415.
- [8] A.B. Rechester, M. N. Rosenbluth Phys. Rev. Lett. **40** (1978) 38.
- [9] L. Spitzer *et al.*, Physical Review **89** (1953) 977.